

## Supporting Information

### The effect of Ag alloying of Cu<sub>2</sub>(Zn,Cd)SnS<sub>4</sub> on the monograin powder properties and solar cell performance

Kristi Timmo<sup>\*a</sup>, Mare Altosaar<sup>a</sup>, Maris Pilvet<sup>a</sup>, Valdek Mikli<sup>a</sup>, Maarja Grossberg<sup>a</sup>, Mati Danilson<sup>a</sup>, Taavi Raadik<sup>a</sup>, Raavo Josepson<sup>b</sup>, Jüri Krustok<sup>b</sup> and Marit Kauk-Kuusik<sup>a</sup>

<sup>a</sup> Department of Materials and Environmental Technology, Tallinn University of Technology, Ehitajate tee 5, 19086 Tallinn, Estonia. E-mail: kristi.timmo@taltech.ee

<sup>b</sup> Division of Physics, Tallinn University of Technology, Ehitajate tee 5, 19086 Tallinn, Estonia

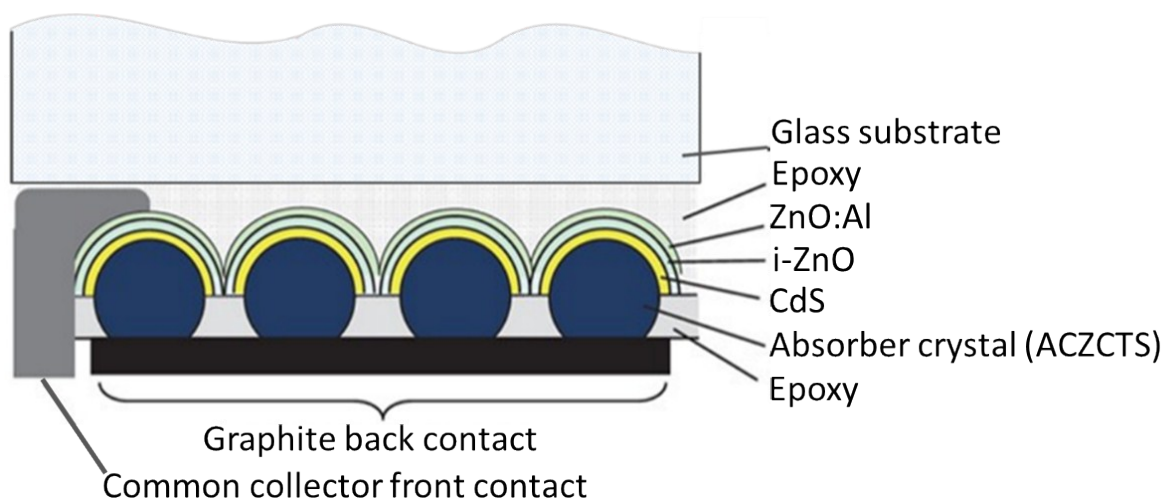


Figure S1. Scheme of monograin layer solar cell structure.

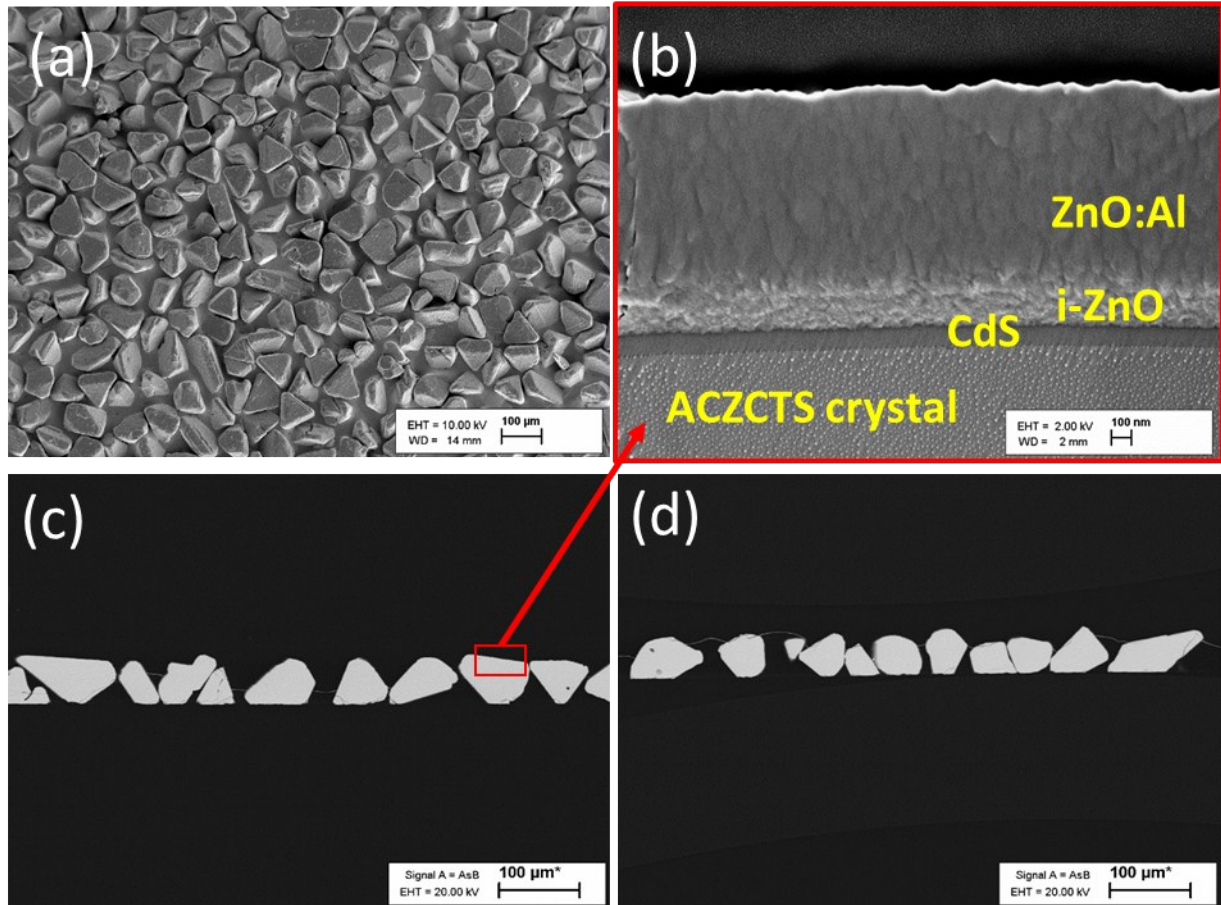


Figure S2. (a) SEM top view of monograin layer membrane and (b) cross-sectionional view of one single ACZCTS crystal in membrane. Polished cross-sectional view of ACZCTS monograin layer solar cells for (c) 0% Ag and (d) 15% Ag.

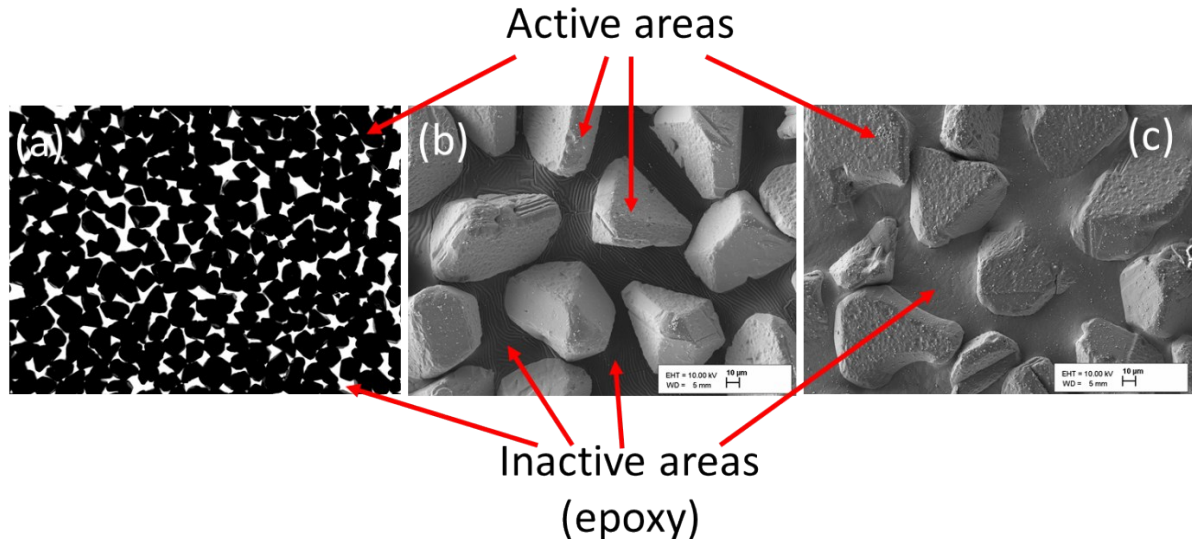


Figure S3. (a) Planar image of the packing density of crystals in the membrane. (b) Top view of membrane, where crystals are half embedded into the epoxy and (c) more than half inside the epoxy.

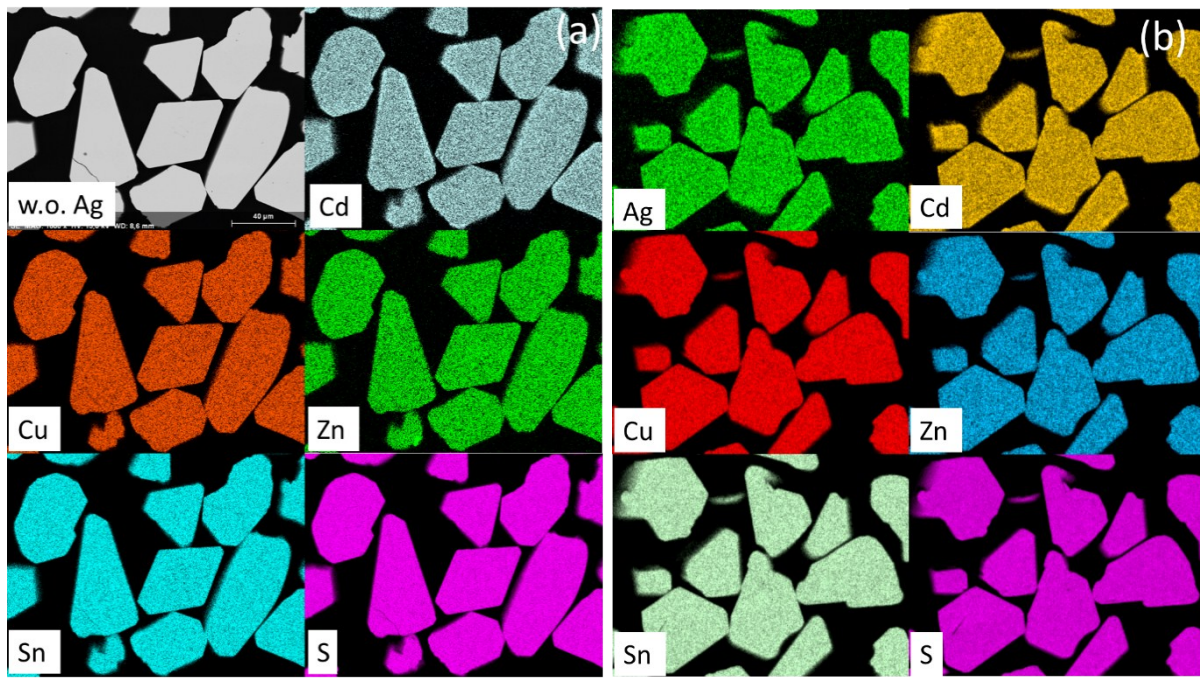


Figure S4. EDX elemental mapping of Ag, Cd, Cu, Zn, Sn and S for as-grown ACZCTS polished crystals with (a) 0% and (b) 1% of input Ag.

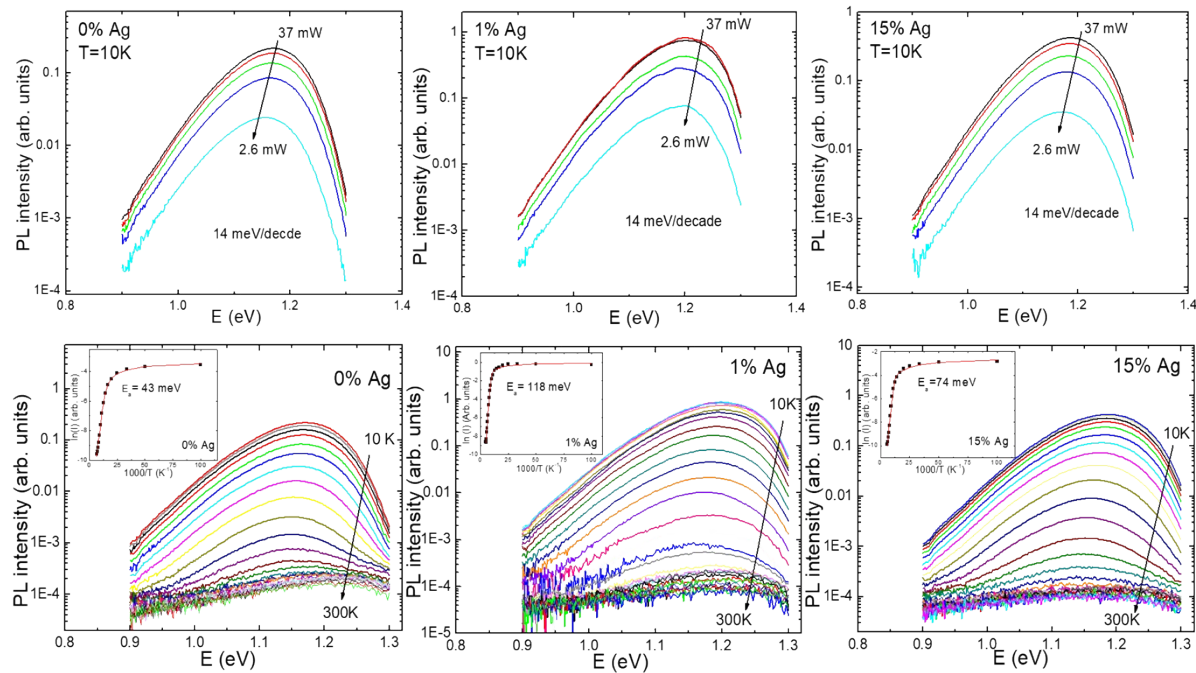


Figure S5. The laser power and temperature dependencies of the PL spectra for  $(\text{Cu}_{1-x}\text{Ag}_x)_{1.85}(\text{Zn}_{0.8}\text{Cd}_{0.2})_{1.1}\text{SnS}_4$  monograin powders with  $x = 0, 1$  and  $15\%$ . The inset graphs present the thermal activation energies derived from the temperature dependencies of the PL spectra.

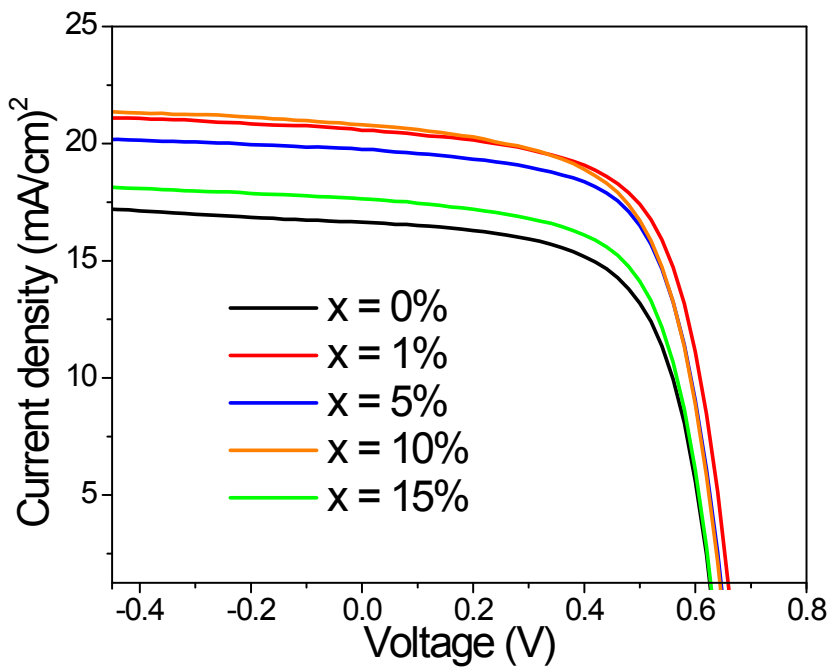


Figure S6. Light  $J$ - $V$  curves of the  $(\text{Cu}_{1-x}\text{Ag}_x)_{1.85}(\text{Zn}_{0.8}\text{Cd}_{0.2})_{1.1}\text{SnS}_4$  solar cells with different added percentages of Ag for Cu substitution ( $x = 0\text{-}15\%$ ).